

# Insights into phase stability of anhydrous/hydrate systems: a Raman-based methodology

Mariela M. Nolasco,<sup>a\*</sup> Ana M. Amado<sup>b</sup> and Paulo J. A. Ribeiro-Claro<sup>a</sup>



FT-Raman spectroscopy turns out to be a powerful technique to evaluate the amount of polymorphic and pseudopolymorphic forms in crystalline samples – which is particularly relevant in pharmaceutical sciences. This paper presents a methodology that allows successful quantitative evaluation of the solid-state hydration and dehydration processes, using FT-Raman spectroscopy. All the steps required for a reliable evaluation of the hydration/dehydration process are illustrated for the caffeine system, a particularly challenging system presenting limited spectral differences between the pseudopolymorphs. The hydration process of caffeine was found to occur in a single-step process with a half-life time of ca 13 h, while the dehydration occurs through a two-step mechanism. The critical relative humidity was found to be at ca 81 and 42% for anhydrous and hydrate caffeine forms, respectively. Copyright © 2009 John Wiley & Sons, Ltd.

Supporting information may be found in the online version of this article.

**Keywords:** Raman spectroscopy; hydration/dehydration; kinetics; phase stability; caffeine

## Introduction

It has long been known that pharmaceutical solids can exist in more than one solid-state crystal form,<sup>[1]</sup> which can have significantly different pharmaceutical properties, such as solubility, dissolution rate and bioavailability.<sup>[2–5]</sup> In addition to polymorphs,<sup>[6,7]</sup> other examples of possible solid states are solvates and hydrates.<sup>[8]</sup>

Different techniques ranging from thermal methods to spectroscopic tools (nuclear magnetic resonance, X-ray diffraction and vibrational spectroscopy) can be applied to monitor pseudopolymorphic transitions.<sup>[9–14]</sup> In the last few years, the investigation of pharmaceutical compounds by means of Raman spectroscopy has attracted much interest, and some exhaustive reports<sup>[15–17]</sup> have pointed out the pharmaceutical applications of Raman spectroscopy. This technique, which provides an excellent method for probing solid-state hydrogen-bonding interactions between molecules (including polymorphs and solvates<sup>[9,10,15,18–23]</sup>), is more often associated with qualitative analysis. However, the application of Raman spectroscopy to monitor the solid-phase composition during polymorphic and pseudopolymorphic phase transitions has been described in recent publications.<sup>[24–35]</sup>

It has been reported that approximately one-third of pharmaceutical solids are capable of forming a hydrate form,<sup>[36]</sup> depending on the environmental conditions (temperature and vapor pressure).<sup>[37]</sup> As the hydration state may affect the physical and chemical properties of the pharmaceutical product,<sup>[4,5]</sup> it is important to know the response of pharmaceutical solids to different environments of storage, namely humidity and temperature conditions, evaluating therefore the solid-state interconversion of such hydrates with their anhydrous forms that dictate the stability of a solid phase.

In order to accomplish this purpose, a Raman spectroscopy methodology is presented and applied for caffeine – used as a model drug. This methodology was found to yield reliable kinetic

data for systems that present large spectral changes between hydrate and anhydrous forms, such as theophylline<sup>[27]</sup> and niclosamide.<sup>[29]</sup> The applicability of the methodology in systems with less evident changes is well illustrated in this study with caffeine.

Caffeine (1,3,7-trimethylpurine-2,6-dione; hereafter called CA, Fig. 1) is a methylated xanthine derivative that naturally occur in food products such as tea, coffee and chocolate and is one example of the many drugs sensitive to polymorphic and pseudopolymorphic transformations.<sup>[38–45]</sup> This compound finds a variety of medical applications, being routinely prescribed, for instance, as a central nervous system stimulant<sup>[46]</sup> and presents beneficial effects in preventing Parkinson and Alzheimer diseases.<sup>[47–49]</sup> CA is also known to cause diuresis,<sup>[50]</sup> and their administration seems to protect mice against whole-body lethal dose of  $\gamma$ -irradiation.<sup>[51]</sup>

The solid-state properties of CA have been widely investigated; it is known to crystallize into different crystalline states, namely as one crystalline nonstoichiometric hydrate,<sup>[40,52,53]</sup> hereafter named as CAh, and a pair of anhydrous  $\alpha$ - and  $\beta$ -polymorphs.<sup>[40,52,54–58]</sup> The anhydrous  $\beta$ -form, hereafter named as CAa (anhydrous CA), is stable at room temperature, whereas the  $\alpha$ -form only occurs at higher temperatures.<sup>[44,45,56,59]</sup>

The present paper has been organized as follows. Firstly, the methodology applied is described. Secondly, the results

\* Correspondence to: Mariela M. Nolasco, CICECO, Chemistry Department, University of Aveiro, P-3810-193 Aveiro, Portugal. E-mail: mnolasco@ua.pt

a CICECO, Chemistry Department, University of Aveiro, P-3810-193 Aveiro, Portugal

b Quimica-Física Molecular, Chemistry Department, FCTUC, University of Coimbra, P-3004-535 Coimbra, Portugal

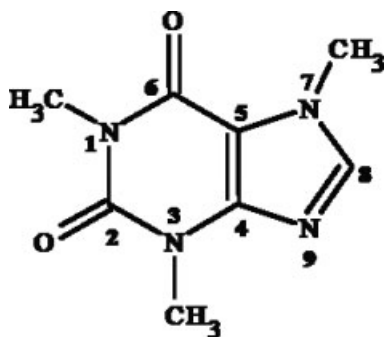


**Figure 1.** Schematic representation of caffeine and atom numbering used in the text.

obtained for the CA system are presented and discussed in four main sections, concerning (1) the selection of the most useful spectral regions; (2) the calibration procedure; (3) the underlying mechanisms and (4) the critical relative humidity (RH) conditions for both hydration and dehydration processes of CA forms.

## Methodology

The Raman spectroscopy methodology here presented is based on the vibrational structural differences observed in most of hydrate/anhydrous systems as a result of the changes in intermolecular contacts. The different spectral Raman features (peak positions and intensities) observed in the spectra of distinct solid-state forms are the key factors that allow monitoring the process during the phase transition.

Water, being a component of the atmosphere which considerably varies from country to country and day to day, is the most critical parameter when substances may transform to hydrates under normal storage conditions. As water will be absorbed and desorbed with temperature and moisture changes, an experimental methodology that accounts for these factors is of utmost importance.

Consider a hygroscopic pharmaceutical anhydrous compound, X<sub>a</sub>, that display facile conversion to a hydrate form, X<sub>h</sub>, by uptake of moisture into a solid dosage form upon equilibration with the ambient environment. Monitoring the amount of X<sub>a</sub> and X<sub>h</sub> forms at different RH and temperature conditions (see below, sample treatment) allows, by using this methodology, the investigation of hydration and dehydration kinetics of pharmaceutical compounds at various conditions of humidity and temperature. Additionally, the possible mechanisms underlying the hydration and dehydration processes of CA forms, as well as the critical RH conditions for both processes, can be determined.

### Quantification anhydrous/hydrate forms by peak area measurements

In order to use Raman spectroscopy in the quantitative evaluation of X<sub>a</sub> and X<sub>h</sub> forms, it is firstly necessary to identify the distinct bands due to the different pseudopolymorphic forms intervening in the reaction pathway, i.e. *reactant* and *product*. Among a given pair of bands ascribed to the *reactant* and *product*, there will be a time-dependent intensity transfer during the reaction.

The selected spectral regions, with spectral differences between anhydrous and hydrate, are evaluated for their suitability to be used in the relative quantification of the two forms. X<sub>a</sub> and X<sub>h</sub> are

function of the time of reaction (X<sub>a</sub> hydration and X<sub>h</sub> dehydration). Two main criteria should be considered. Firstly, the existence of an isobestic point is required. Secondly, the number of bands required for the spectral deconvolution process should be the lowest to avoid 'over-parameterization' errors.

1. Different pseudopolymorphic forms (X<sub>a</sub> and X<sub>h</sub>) give rise to different Raman bands. The observed intensity of the band associated with a given pseudopolymorphic form ( $I_{X_a}$  and  $I_{X_h}$ ) is directly proportional to the intrinsic intensity of the corresponding vibrational mode ( $\delta_{X_a}$  and  $\delta_{X_h}$ ) and to the relative concentration of that pseudopolymorphic form in the sample ( $C_{X_a}$  and  $C_{X_h}$ ):

$$I_{X_a} = \delta_{X_a} \times C_{X_a} \quad (1)$$

$$I_{X_h} = \delta_{X_h} \times C_{X_h} \quad (2)$$

Additionally, the presence of a pseudo-isobestic point in a specific spectral region of the Raman spectra is an indication that only two species exist in equilibrium and that they interconvert directly.<sup>[60,61]</sup> Therefore, the Raman data can be converted to a normalized form, called fractional of conversion ( $\alpha$ ), that ranges from 0 to 1 and is a measure of the progress of the reaction, in terms of intensity transfer from one band to the other, as a function of time.

In order to apply the above procedure, it is necessary to determine the calibration relationships so that the relative proportions of hydrate ( $\alpha_h$ ) and anhydrous ( $\alpha_a$ ) in the samples could be determined without doubt. In fact, the relative intrinsic intensity of a particular mode may differ significantly depending on the considered pseudopolymorphic form. By preparing physical mixtures with well-known molar fractions ratio, the relative intrinsic intensities ( $\delta_{X_h}/\delta_{X_a}$  and  $\delta_{X_a}/\delta_{X_h}$ ) of the considered vibrational mode can be determined by linear fitting of the predicted relative intensities (obtained by band deconvolution procedures) as a function of the known molar fractions ratio:

$$\frac{I_{X_a}}{I_{X_h}} = \frac{\delta_{X_a}}{\delta_{X_h}} \times \frac{\chi_{X_a}}{\chi_{X_h}} \quad (3)$$

where  $\chi_{X_a}$  and  $\chi_{X_h}$  are the mole fraction of the anhydrous and hydrate forms, respectively.

After the determination of the relative intrinsic intensities of the considered vibrational mode, the values of the fractional of hydration ( $\alpha_h$ ) and of dehydration ( $\alpha_a$ ) at a particular time of reaction  $t$  (time of exposure to RH conditions or time of storage at a given temperature) can be determined as

$$\alpha_h(t) = I_{X_h} / [I_{X_h} + (\delta_{X_h}/\delta_{X_a})I_{X_a}] \quad (4)$$

and

$$\alpha_a(t) = I_{X_a} / [I_{X_a} + (\delta_{X_a}/\delta_{X_h})I_{X_h}] \quad (5)$$

respectively. By definition,  $\alpha_h + \alpha_a = 1$ .

### Determination of kinetic parameters

One crucial step in any kinetic study is finding the mechanism for the rate-determining reaction step that gives the best description of the studied process, and ultimately allows calculating meaningful kinetic parameters. In this context, once the fractional of conversion ( $\alpha_h$  and  $\alpha_a$ ) has been obtained, a set of kinetics parameters concerning the hydration and dehydration processes can be obtained by fitting different models to the data, which allow

**Table 1.** Solid-state reaction rate equations and mechanisms<sup>[62–65]</sup>

Model	Equation, $f(\alpha) = kt^a$	Rate-controlling mechanism
M1	$\alpha^{1/4}$	Power law
M2	$\alpha^{1/3}$	Power law
M3	$\alpha^{1/2}$	Power law
M4	$\alpha^{3/2}$	Power law
M5	$1 - \alpha$	One-dimensional phase boundary reaction (zero-order)
M6	$1 - (1 - \alpha)^{1/2}$	Two-dimensional phase boundary reaction (cylindrical symmetry)
M7	$1 - (1 - \alpha)^{1/3}$	Three-dimensional phase boundary reaction (spherical symmetry)
M8	$-\ln(1 - \alpha)$	Random nucleation (Mampel equation)
M9	$(-\ln(1 - \alpha))^{1/2}$	Random nucleation (Avrami–Erofeev equation; $n = 1/2$ )
M10	$(-\ln(1 - \alpha))^{1/3}$	Random nucleation (Avrami–Erofeev equation; $n = 1/3$ )
M11	$(-\ln(1 - \alpha))^{1/4}$	Random nucleation (Avrami–Erofeev equation; $n = 1/4$ )
M12	$(-\ln(1 - \alpha))^{2/3}$	Random nucleation (Avrami–Erofeev equation; $n = 2/3$ )
M13	$\alpha$	Zero-order mechanism (Polanyi–Wigner equation)
M14	$\alpha^2$	One-dimensional diffusion
M15	$(1 - \alpha) \ln(1 - \alpha) + \alpha$	Two-dimensional diffusion
M16	$(1 - (1 - \alpha)^{1/3})^2$	Three-dimensional diffusion (Jander equation)
M17	$1 - (2\alpha/3) - (1 - \alpha)^{2/3}$	Three-dimensional diffusion (Ginstling–Brounshtein equation)

<sup>a</sup>  $\alpha$  stands for  $X_a \rightarrow X_h$  or  $X_h \rightarrow X_a$  degree of conversion;  $k$  is the rate constant of the conversion reaction;  $t$  is time of exposure to RH conditions or time of storage at a given temperature.

identifying the mechanism underlying both  $X_a \rightarrow X_h$  and  $X_h \rightarrow X_a$  conversions. Different kinetic models  $f(\alpha) = kt$  have been proposed for characterizing the solid-state reaction mechanisms, such as the present pseudopolymorphic conversions (Table 1).<sup>[62–65]</sup> Some examples of hydration and dehydration kinetics studies described by such models can be found in the literature.<sup>[64,66]</sup> For example, dehydration of calcium oxalate monohydrate<sup>[67]</sup> was shown to follow geometrical contraction models (M6 and M7 kinetic models of Table 1).

### Spectral band deconvolution and mathematical data treatment

For the evaluation of band intensity ratios, the integrated band intensities ( $I_{X_h}$  and  $I_{X_h}$ ) can be determined by band-fitting procedures, using two Gaussian or two Lorentzian functions, after performing a linear baseline correction employing three points. For the determination of pseudo-isosbestic points, the procedure described by Girling and Shurvell<sup>[60]</sup> and Pemberton and Shurvell<sup>[61]</sup> should be considered.

Different standard statistical criteria may be used to determine the aggregate deviation of a set of measured points from the calculated linear relationship. The most usually used are the correlation coefficient ( $R^2$ ) and the standard error of the slope of the regression line ( $s_b$ ). Some authors<sup>[62,68]</sup> have reported the inadequacies of using  $r$ -value as the sole determinant of the applicability of a particular kinetic model, particularly for distinguishing between mechanism that yield similar linear correlation coefficients ( $R^2$ ). Davies and Pryor<sup>[68]</sup> pointed out the advantages of using  $s_b$  values instead. In this work, the quality of the linear fit obtained for each kinetic model tested (Table 1) is determined by considering both  $R^2$  and  $s_b$  values.

## Experimental

### Materials

CAa was obtained commercially (Sigma-Aldrich) and used without further purification (grain size between 125 and 250  $\mu\text{m}$ ). Hydrate CA (CAh) was prepared by dissolving CAa in distilled water at 80 °C until a supersaturated solution is prepared. When the solution was allowed to slowly cool to room temperature, the crystals that formed were filtered from the mother liquid, allowed to dry at ambient temperature and then gently milled to a fine powder (grain size between 125 and 250  $\mu\text{m}$ ). As CAh when exposed to ambient conditions, even for a short time period, tend to undergo partial dehydration, the fine powder was stored in a sealed vessel at 92% RH in the presence of a saturated solution of potassium nitrate.

### Sample treatment

In order to monitor the hydration and dehydration kinetics by Raman spectroscopy, different types of experiments were performed. In a first type of experiment, both anhydrous  $\rightarrow$  hydrate and hydrate  $\rightarrow$  anhydrous phase transitions were induced by defined RH and studied at 22 °C ambient temperature. CAa (commercial powder) and CAh samples (ca 0.1 g) were transferred to sealed vessels and exposed, for different time intervals, to the water atmosphere of 100 and 0% RH (without direct contact between the sample and the bulk liquid, Fig. 2), by considering pure water and anhydrous  $\text{CuSO}_4$ , respectively. In a second type of experiment, the dehydration process was promoted by storing the CAh samples at different temperatures (35, 45 and 60 °C) for different time periods, under ambient RH conditions. In both the experiments, after the defined time intervals of exposure, the FT-Raman spectra of the different samples were recorded.

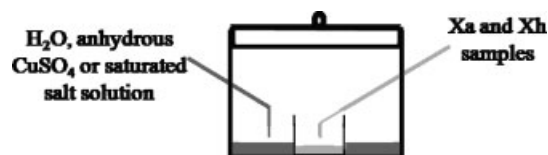


**Figure 2.** Schematic representation of the reservoir used for sample exposure to specific RH values.

For the purpose of providing the critical RH values for both the anhydrous and hydrate forms, CAa and CAh samples (*ca* 0.1 g) were exposed to different RH conditions. To control RH conditions, saturated salt solutions with deposits were used. The RH values considered (and salt used) were taken from Ref. [69] and were as follows: 9% (KOH), 13% (LiCl), 20% (KC<sub>2</sub>H<sub>3</sub>O<sub>2</sub>), 30% (CaCl<sub>2</sub>), 42% (Zn(NO<sub>3</sub>)<sub>2</sub>), 48% (KCNS), 52% (NaHSO<sub>4</sub>), 58% (NaBr), 61% (NH<sub>4</sub>NO<sub>3</sub>), 66% (NaNO<sub>2</sub>), 78% (Na<sub>2</sub>SO<sub>3</sub>), 79% (NH<sub>4</sub>Cl), 81% ((NH<sub>4</sub>)<sub>2</sub>SO<sub>4</sub>), 84% (KBr), 86% (KHSO<sub>4</sub>) and 92% (KNO<sub>3</sub>). In all cases, the exposure time of the sample at the considered RH was 1 week in order to guarantee the equilibrium moisture condition. After that period of exposure, the FT-Raman spectra of the different samples were recorded. All experiments were performed at ambient temperature.

In order to determine the calibration relationship, physical mixtures of CAh/CAa with known compositions (CAh molar fractions of 0.00, 0.155, 0.165, 0.222, 0.500, 0.751 and 1.00) were prepared by smoothly mixing the samples in a mortar for 2 min to ensure mixing uniformity. Effects of particle size were examined by manually sieving samples to give particle size ranges between 125 and 250  $\mu\text{m}$ .

### FT-Raman spectroscopic experiments

The FT-Raman spectra were recorded on an RFS-100 Bruker FT-spectrometer, using a Nd:YAG laser with excitation wavelength of 1064 nm, with laser power set to 300 mW. Each spectrum is the measurement of 100 scans with 2  $\text{cm}^{-1}$  resolution. As emphasized in our previous work,<sup>[27]</sup> it is apparent that in some experiments the sample temperature can rise significantly due to laser exposure<sup>[70,71]</sup> and promote either loss of solvent molecules or polymorphic transformations. For the purpose of evaluating

this effect, a sample of CAh was exposed continuously to 500 mW laser power for approximately 1 h and 40 min, and 20 records of 5 min each were collected. All the FT-Raman spectra reported on this work (using the conditions described above) have been collected in 25 min or less, after which period no spectral changes assignable to sample heating were observed on the exposure of CAh to the laser.

## Results and Discussion

### Selection of the most useful spectral regions

Figure 3 compares the Raman spectra of CAa and CAh forms in the 100–1800  $\text{cm}^{-1}$  and 2700–3400  $\text{cm}^{-1}$  spectral regions. Selecting a suitable region for quantitative analysis would initially appear difficult since the FT-Raman spectra have very similar patterns, reflecting minor changes in the molecular vibrations due to different packing arrangements of the molecules.

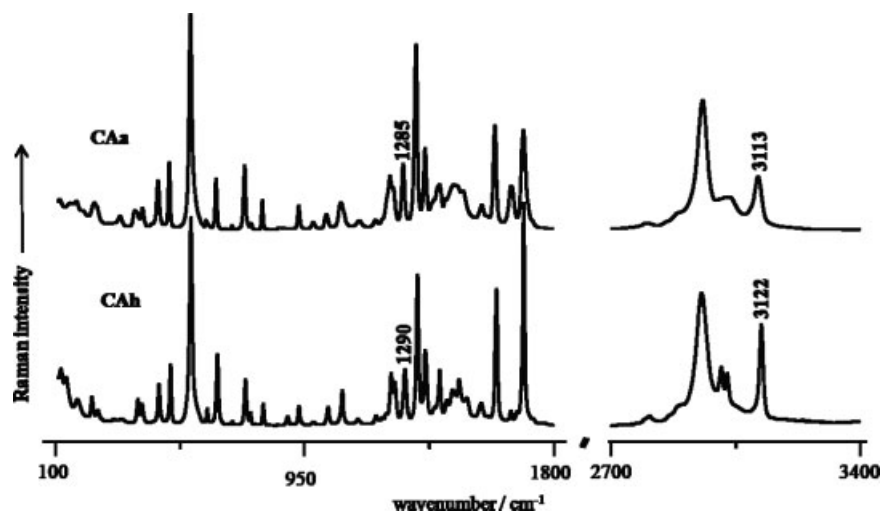
The spectral regions labeled with wavenumbers in Fig. 3 were found to be the most amenable for the present study, according to the criteria defined above: each pair presents a pseudo-isosbestic point and can be described in the spectral deconvolution process by only two single bands, avoiding the ‘over-parameterization’ errors.

According to our previous study,<sup>[72]</sup> these are related to the stretching mode of the oscillators C<sub>8</sub>–H (3070–3150  $\text{cm}^{-1}$ ) and CC + CN (1270–1310  $\text{cm}^{-1}$ ). In the remaining regions, only slight intensity changes are observed. The complete vibrational assignment can be found in the reported study.<sup>[72]</sup>

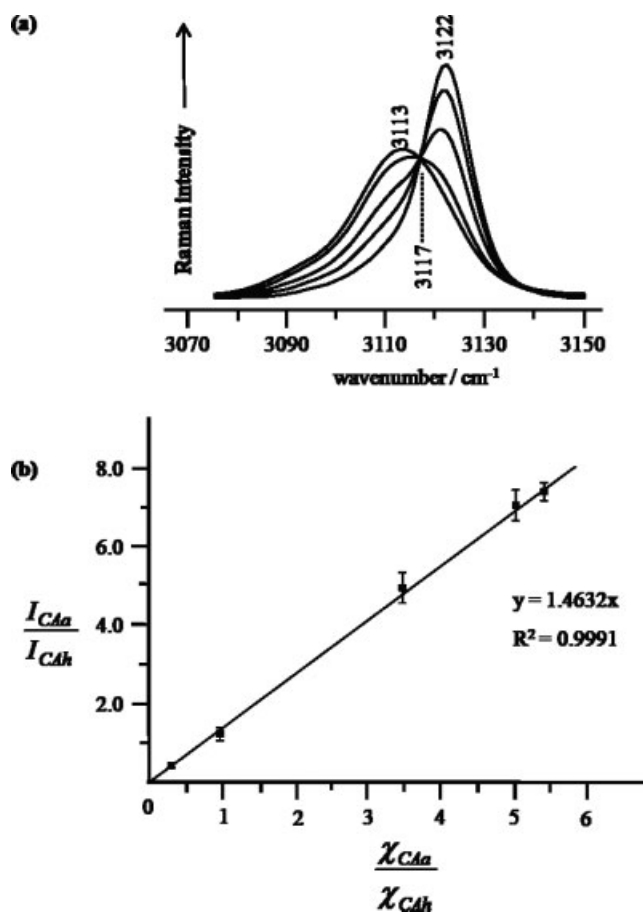
### Calibration procedure

Figure 4 summarizes the calibration procedure for the stretching mode of the oscillators C<sub>8</sub>–H (3070–3150  $\text{cm}^{-1}$ ). Figure 4(a) shows that this spectral region presents an isosbestic point at 3117  $\text{cm}^{-1}$ . Figure 4(b) shows the plot of  $I_{\text{CAa}}/I_{\text{CAh}}$  versus  $\chi_{\text{CAa}}/\chi_{\text{CAh}}$  used to evaluate the required ratio  $\delta_{\text{CAa}}/\delta_{\text{CAh}}$ . This calibration procedure was also made for the 1270–1310  $\text{cm}^{-1}$  spectral region, and the results are summarized in Table 2.

The comparison between the FT-Raman spectra of CAa (solid line) and CAh (dashed line) forms in the 1270–1310 and



**Figure 3.** FT-Raman spectra of CAa and CAh in the 100–1800  $\text{cm}^{-1}$  and 2700–3400  $\text{cm}^{-1}$  spectral regions. Some bands showing the most pronounced differences between CA forms are marked.



**Figure 4.** Calibration procedure. (a) FT-Raman spectra, in the 3070–3150  $\text{cm}^{-1}$ , of physical mixtures of CAa and CAh with well-known composition (CAh molar fractions of 0.00, 0.155, 0.165, 0.222, 0.500, 0.751 and 1.00 were used). A pseudo-isosbestic point is observed at 3117  $\text{cm}^{-1}$ ; (b) plot of  $I_{\text{CAa}}/I_{\text{CAh}}$  versus  $X_{\text{CAa}}/X_{\text{CAh}}$  (error bars included).

3070–3150  $\text{cm}^{-1}$  spectral regions, after scaling in order to reflect their relative intrinsic intensities, is shown in Fig. 5.

### Mechanisms underlying hydration/dehydration processes of CA forms

The dehydration process of CAh has been studied in detail,<sup>[40–43,52,73,74]</sup> but significantly less research has been done on the reverse process, from anhydrous caffeine to hydrate caffeine.<sup>[43,74]</sup>

### Mechanism for the CAa→CAh process

The kinetics of anhydrous conversion from CAa to CAh by exposure to water-saturated atmosphere were monitored as described in the experimental section. Figure 6(a) and (b) show the sequential change of the CC + CN stretching mode (1270–1310  $\text{cm}^{-1}$  region) and the plot of the measured fractional of hydration ( $\alpha_h$ ) as a function of time of exposure to RH = 100% conditions at 22 °C. The time-dependent intensities observed in the 3070–3150  $\text{cm}^{-1}$  spectral region present a similar behavior.

The steepest increase is observed around ca 960 min (16 h), and after 25 h of exposure the anhydrous form was totally transformed to the hydrate (situation referred to in Fig. 6(a) as CAh), which is in accordance with the results of X-ray diffraction and hygroscopicity measurements published by Pirttimäki and Laine.<sup>[43]</sup> Larger times of exposure did not give rise to any further observable spectral change.

The fractional of hydration ( $\alpha_h$ ) measured for the two considered regions were fitted to the different kinetic models listed in Table 1, in order to choose the model giving the best statistical fit. As already emphasized in this work, the most usually used statistical criteria are the correlation coefficient ( $R^2$ ) and the standard error of the slope of the regression line ( $s_b$ ). Thus, the quality of the linear fit obtained for the different kinetic models was determined by considering both of them (Table S1, Supporting Information). Table 3 shows the best kinetic results obtained for CAa hydration.

Although the  $R^2$  and  $s_b$  values for M9 and M13 kinetic models are somewhat similar (Table 3), M9 was assumed to yield a better description of the overall results (two spectroscopic regions). Within this assumption, it was found that the hydration of CAa follows a *one-step random nucleation process*, described by the Avrami–Erofeev equation of exponent 1/2 with a rate constant of ca  $(1.14 \pm 0.05) \times 10^{-3} \text{ min}^{-1}$ . The time required for half-hydration ( $t_{1/2}$ ) was ca 750 min ( $\approx 13$  h) with the completion of CAa hydration after ca 3030 min ( $\approx 51$  h).

Although these results are not in accordance with the studies of Pirttimäki and Laine,<sup>[43]</sup> which suggest that CAa hydration involves two steps with a 50% hydration achieved after 26 h, these discrepancies can be explained by the different history of the CAa samples used. In this work, commercial CAa samples were used, while in the reported study<sup>[43]</sup> the CAa samples were obtained by dehydration of CAh samples. This situation can lead to significantly different samples morphologies (e.g. grain size and crystal defects), which can affect the hydration behavior.

### Mechanism for the CAh→CAa process

The kinetics of the conversion of CAh to CAa by exposure to very low water vapor pressure conditions were monitored. Figure 7(a)

**Table 2.** Results obtained for the plot of  $I_{\text{CAa}}/I_{\text{CAh}}$  versus  $X_{\text{CAa}}/X_{\text{CAh}}$

Spectral region	Vibrational mode <sup>a</sup>	Band centre (wavenumbers in $\text{cm}^{-1}$ )		$b^b$	$s_b^b$	$R^{2b}$	$\frac{\delta_{\text{CAa}}}{\delta_{\text{CAh}}}$
		CAa	CAh				
3070–3150 $\text{cm}^{-1}$	$\nu_{\text{C}=\text{O}}$	3113	3122	1.4632	0.14057	0.9991	1.46
1270–1310 $\text{cm}^{-1}$	$\nu_{\text{CC}} + \nu_{\text{CN}}$	1285	1290	0.6147	$8.27 \times 10^{-2}$	0.9922	0.62

<sup>a</sup> In accordance with Ref. [72];  $\nu$  stands for stretching.

<sup>b</sup>  $b$  and  $s_b$  stand for slope and slope standard deviation of the linear regression line, respectively;  $R^2$  for the correlation coefficient;  $\delta_{\text{CAh}}$  and  $\delta_{\text{CAa}}$  stand for intrinsic intensities of the mode for the CAh and CAa forms, respectively.

# Explore Litigation Insights

Docket Alarm provides insights to develop a more informed litigation strategy and the peace of mind of knowing you're on top of things.

## Real-Time Litigation Alerts



Keep your litigation team up-to-date with **real-time alerts** and advanced team management tools built for the enterprise, all while greatly reducing PACER spend.

Our comprehensive service means we can handle Federal, State, and Administrative courts across the country.

## Advanced Docket Research



With over 230 million records, Docket Alarm's cloud-native docket research platform finds what other services can't. Coverage includes Federal, State, plus PTAB, TTAB, ITC and NLRB decisions, all in one place.

Identify arguments that have been successful in the past with full text, pinpoint searching. Link to case law cited within any court document via Fastcase.

## Analytics At Your Fingertips



Learn what happened the last time a particular judge, opposing counsel or company faced cases similar to yours.

Advanced out-of-the-box PTAB and TTAB analytics are always at your fingertips.

## API

Docket Alarm offers a powerful API (application programming interface) to developers that want to integrate case filings into their apps.

## LAW FIRMS

Build custom dashboards for your attorneys and clients with live data direct from the court.

Automate many repetitive legal tasks like conflict checks, document management, and marketing.

## FINANCIAL INSTITUTIONS

Litigation and bankruptcy checks for companies and debtors.

## E-DISCOVERY AND LEGAL VENDORS

Sync your system to PACER to automate legal marketing.